1

On the Role of Battery Energy Storage Systems in the Day-Ahead Contingency-Constrained Unit Commitment Problem under Renewable Penetration

Alexandre Moreira[a,*], Bruno Fanzeres[b], Patricia Silva[c], Miguel Heleno[a], André Luís Marques Marcato[c]

[a]*Lawrence Berkeley National Laboratory, 1 Cyclotron Rd, Berkeley, CA 94720, USA.*
[b]*Industrial Engineering Department, Pontifical Catholic University of Rio de Janeiro (PUC-Rio), Rio de Janeiro, RJ, Brazil.*
[c]*Federal University of Juiz de Fora (UFJF), Campus Universitário, Rua José Lourenço Kelmer, s/n - São Pedro, Juiz de Fora - MG, 36036-900, Brazil.*

Abstract

The integration of variable Renewable Energy Sources (vRES) to alleviate greenhouse gas emissions has introduced significant challenges for power systems operations. These challenges include high levels of uncertainty due to the intermittence associated with vRES and therefore impose the need to devise a reliable and cost-effective day-ahead unit commitment and power and reserves scheduling for real-time operations. Also, this increasing penetration of vRES requires higher ramping capabilities from units originally designed for other purposes (e.g., base-load generation), which might be exacerbated during contingency states. Hence, in this work, we propose a methodology to address the day-ahead Contingency-Constrained Unit Commitment (CCUC) problem that leverages the participation of Battery Energy Storage Systems (BESSs) to address load-following and post-contingency management, therefore alleviating the ramping burden on conventional thermal generators. To do so, we formulate a three-level optimization problem that represents the decision-making process of obtaining the least-cost commitment, generation and reserves scheduling, while restricting the Conditional Value-at-Risk (CVaR) of the system imbalance at real-time operations to user-defined tolerance levels. In addition, we devise a computationally efficient solution approach for the proposed problem based on the Column-and Constraint Generation (CCG) algorithmic framework. Two numerical experiments are conducted to empirically illustrate the benefits of the proposed methodology. Key results indicate a reduction in real-time ramping needs and a better usage of the system resources, with a reduction in the overall system commitment levels and reserve scheduling costs when compared to a benchmark case in which storage is not available.

Keywords: Column-and-Constraint Generation; Conditional Value-at-Risk; Day-Ahead Scheduling; Energy Storage Systems; Security Criterion; and Renewable Energy.

1. Introduction

Several countries around the globe have agreed to reduce greenhouse gas emissions in their economic sectors and supply chains to deal with climate changes and therefore deliver key long-term environmental safety to society [1]. In the particular context of power systems, this agreement is currently being fulfilled

[1]This study was partially supported by the Coordenação de Aperfeiçoamento de Pessoal de Nível Superior – Brasil (CAPES) – Finance Code 001. Bruno Fanzeres gratefully acknowledges the financial support from CNPq, project 309064/2021-0, and FAPERJ, project E-26/202.825/2019.

*Corresponding author.
Email addresses: AMoreira@lbl.gov (Alexandre Moreira), bruno.santos@puc-rio.br (Bruno Fanzeres), patricia.sousa@engenharia.ufjf.br (Patricia Silva), MiguelHeleno@lbl.gov (Miguel Heleno), andre.marcato@ufjf.edu.br (André Luís Marques Marcato)

through the replacement of conventional thermal generators by variable Renewable Energy Sources (vRES) [2, 3]. However, due to the weather-dependence of vRES supply, this replacement has a profound and structural impact on the decision-making process of power systems planning and operations. In California, for instance, the intermittence of vRES and the provision of reserves to deal with outages are usually addressed by conventional generators such as the gas-fired generation units. As renewable penetration progresses, the observations of high ramping levels provided by conventional generation sources becomes recurrent [4]. However, as also mentioned in [4], some of these gas-fired units (especially those that operate on combined cycles) were designed to serve as base-load generation, thus more frequent fast starts, cycling and load-following ancillary services can cause their early retirement. In addition, Senate Bill 100 [5] imposes high targets of renewable penetration for the forthcoming decades (60% by 2030 and 100% by 2045). These targets might further increase the need for an alternative to replace gas-fired generation in the role of dealing with vRES intermittence and providing contingency reserves.

A potential alternative to cope with these issues is the deployment of Battery Energy Storage Systems (BESSs) in power systems [6, 7, 8, 9]. Essentially, BESSs can smooth the energy demand and shift the supply throughout the time horizon, thus relieving load-following units from providing high ramping levels. Furthermore, they can provide clean and economic ancillary services against uncertain supply and unplanned system's components unavailability with high ramping rates in real-time operation, and potentially deffer investments in transmission capacity, avoiding, for instance, network over-sizing [10, 11]. However, it is still unclear how system operators should model the participation of BESSs in day-ahead electricity markets so as to leverage these assets to the highest extent to provide energy and provision of reserves, therefore benefiting the end-users with a reliable and environmentally-friendly service.

Hence, in this paper, we propose a novel methodology to determine, from the point of view of the system operator, a cost-effective day-ahead scheduling of the system while leveraging BESSs to ensure a reliable real-time operation. Methodologically, the proposed day-ahead scheduling process fits within the class of hierarchical optimization problems and is formulated as a three-level system of mathematical programming models. Structurally, the first-level model describes the day-ahead scheduling process that aims (i) to identify an operating point with the least-cost level under an *a-priori*-defined nominal condition and (ii) to comply with a system imbalance restriction to a maximum user-defined acceptable level through Conditional Value-at-Risk (CVaR) [12] functionals. Then, for a given scenario of renewable output realization, the second-level problem emulates the deterministic security standard setup and identifies a contingency state within an *a-priori*-defined set of credible ones that induces the highest system imbalance level, adjusted by the optimal deployment (through a third-level problem) of the conventional and storage reserves over the operating point scheduled in the first-level. It is worth highlighting that this multi-level problem is a non-convex optimization model, thus not suitable for the direct application of standard mathematical programming techniques. Therefore, in this work, we also devise an efficient solution approach by firstly reducing the tri-level structure to a single-level, semi-infinite optimization model, by means of the dual representation of the CVaR risk functional, and then by adapting the Column-and-Constraint Generation (CCG) [13] algorithmic

framework to the resulting single-level optimization model.

Two numerical experiments are conducted to empirically illustrate the benefits of the proposed methodology. In both case studies, the main results indicate a reduction in the need of ramping from conventional generators in real-time operation and a better usage of the system resources, with a reduction in commitment and reserve costs when compared to the same system without storage.

Overall, the main contributions of this work can thus be summarized as follows.

1. To formulate a two-stage day-ahead scheduling problem to determine the power and reserves provided by conventional thermal units and storage devices with the least cost under an *a-priori*-defined nominal condition, while restricting the CVaR of the system imbalance at real-time operations to user-defined tolerance levels. The proposed scheduling framework is formulated as a three-level system of mathematical programming models. Two of the most critical uncertainties in power system planning and operations are accounted for: (i) vRES output by leveraging a data-informed decision-making process with a collection of exogenously-defined scenarios; and (ii) potential failures of system elements using a deterministic security criterion through robust optimization techniques.
2. To devise a computationally efficient solution approach for the proposed day-ahead scheduling problem based on a two-step reformulation procedure: (i) reduction of the three-level system of mathematical programming models into a single-level, semi-infinite one, via the dual representation of the CVaR risk functional and (ii) the design of a tailored Column-and-Constraint Generation (CCG) algorithm that aims to iteratively identify a reduced and finite number of structural blocks of the infinite-scale single-level model that are necessary and sufficient to characterize the feasible region of the problem.

The paper is laid out as follows. Section 2 discusses related work. Section 3 presents the mathematical formulation for the day-ahead power and reserves scheduling problem provisioned by conventional thermal units and storage devices as a three-level system of optimization models. Section 4 thoroughly describes the a solution methodology to efficiently handle the proposed day-ahead scheduling problem. In Section 5, the effectiveness of the proposed model is demonstrated through two numerical experiments comprising an illustrative 5-Bus System and a case study based on the WECC-240 System. Lastly, Section 6 draws the key conclusions of this work.

2. Related Work

Various methodologies have been presented in the literature over the recent years to address the day-ahead scheduling problem under uncertainty, with stochastic programming and robust optimization techniques being the most popular modeling frameworks [14]. In the particular context of considering BESSs, [10, 15, 16] focus on the role of storage devices in load following to accommodate the variation of renewable units, meanwhile [17] and [18] emphasize the potential participation of storage devices in post-contingency corrective measures without accounting for renewable uncertainty. In addition, [19] discusses new storage formulations and provide an extensive computational performance analysis of their general impact in solving the security constrained

unit commitment problem. Furthermore, in power grids with a generation mix predominantly dominated by hydraulic sources, large-scale reservoirs can play an instrumental storage-like role in providing flexibility as discussed in [20].

In fact, adequate schedulings of energy and reserves requirements are of critical importance for the well-functioning of electricity markets [21, 22] and a market structure to properly integrate the participation of BESSs is yet to be designed [23, 24]. A number of works in the literature proposed ways to address this task. In [25], the authors tackle the challenge of securing a reserve scheduling of pumped-storage hydropower units (in a day-ahead unit commitment stage) that is feasible to be deployed without violating state-of-charge limits over time. In addition, [26] explores the potential capabilities of BESSs to provide valuable grid services in a scenario-based stochastic programming framework to address the unit commitment problem, where the scenarios correspond to different realizations of renewable power output and demand consumption. In [27], two multi-stage stochastic models are formulated to determine the scheduling of thermal units and storage charging/discharging power under uncertainty in renewable generation. Based on a usual European electricity market setting, the authors of [28] propose a methodology to schedule energy and reserves for generators and storages while considering uncertainty in renewables and neglecting potential failures in the system. Similarly, another scheduling approach is presented in [29] to assess the flexibility provided by energy storage through different balancing services and the method presented in [30] schedules reserves from pumped hydro storage to deal with renewable intermittence. Moreover, it is important to ensure that reserves provisioned by BESSs can actually be delivered as pointed out by ERCOT in a recent Nodal Protocol Revision Request [31].

Nonetheless, uncertainties associated with renewable generation output and failures of system elements are among the main concerns to the reliable operation of modern and future power systems [14] and the combination of these sources of uncertainty can lead to even more challenging situations. Despite the relevance of the present technical literature, to the best of our knowledge, current works so far only focus on either renewable intermittence or potential contingencies and do not propose a risk-averse approach to deal with these two sources of uncertainties simultaneously while considering the management of BESSs. Thus, the role of the BESSs in energy and reserves co-optimization under this combination of uncertainties has not been properly defined and leveraged. Indeed, the consideration of this combination of uncertainties is very challenging since, for each potential outage, all credible outputs of renewable generation should be taken into account, which results in a highly combinatorial problem with an infinite number of scenarios and constraints. Therefore, in this paper, to fill this gap in the literature, we develop a tailored two-stage risk-averse decision-making framework and propose an effective solution methodology to devise a cost-effective day-ahead power and reserves scheduling for generating units and BESSs under uncertainty in both vRES output and outages of system elements. Our methodology circumvents computational tractability issues by strategically selecting a reduced subset of uncertainty realization scenarios that is sufficient to obtain the optimal solution to the original problem.

3. Mathematical Formulation

The main objective of this work is to propose an efficient methodology to devise a cost-effective thermal and storage power and reserves scheduling for day-ahead operations under uncertainty in both vRES output and failure of system elements (i.e., conventional generators and network transmission lines). To tackle this challenge, a two-stage decision-making process is considered, formulated as a three-level system of mathematical programming models to characterize the thorough decision-making process of a day-ahead operation planning (first stage) along with the reliable energy delivery operation (second stage). Next, the proposed mathematical formulation is presented with Subsection 3.1 describing the day-ahead scheduling model under uncertainty and Subsection 3.2 describing the system operation problem.

3.1. Day-Ahead Thermal and Storage Power/Reserve Scheduling Problem

The proposed day-ahead operation planning model for scheduling power and reserves of thermal and storage units under uncertainty in vRES output and system components availability is presented in (1)–(16) to be described in the next subsections, where $\mathbf{x}^G \triangleq \{\boldsymbol{p}, \boldsymbol{r}^{\text{UP}}, \boldsymbol{r}^{\text{DW}}\}$ and $\mathbf{x}^S \triangleq \{\boldsymbol{v}, \overline{\boldsymbol{z}}, \underline{\boldsymbol{z}}, \overline{\text{r}}, \underline{\text{r}}\}$. Structurally, problem (1)–(16) is a non-convex optimization problem that aims to determine the multi-period day-ahead least-cost scheduling of power and reserves that meets a nominal net consumption and ensures that the system power imbalance is restricted to an *a priori* defined level at each operating hour.

3.1.1. Objective function

$$\underset{\substack{\boldsymbol{p},\boldsymbol{u},\boldsymbol{r}^{\text{UP}},\boldsymbol{r}^{\text{DW}},\\ \boldsymbol{v},\overline{\boldsymbol{z}},\underline{\boldsymbol{z}},\overline{\text{r}},\underline{\text{r}},\\ \boldsymbol{f},\boldsymbol{\theta},\boldsymbol{c}^{\text{SU}},\boldsymbol{c}^{\text{SD}}}}{\text{Minimize}} \sum_{t\in\mathcal{T}}\Bigg(\sum_{i\in\mathcal{I}}\Big(\mathscr{C}_i^G(\boldsymbol{p}_i,\boldsymbol{u}_i) + c_{i,t}^{\text{SU}} + c_{i,t}^{\text{SD}} + c_{i,t}^{\text{UP}} r_{i,t}^{\text{UP}} + c_{i,t}^{\text{DW}} r_{i,t}^{\text{DW}}\Big) + \sum_{h\in\mathcal{H}}\Big(\mathscr{C}_h^S\big(\boldsymbol{v}_h,\overline{\boldsymbol{z}}_h,\underline{\boldsymbol{z}}_h\big) + \overline{\text{c}}_{h,t}\overline{\text{r}}_{h,t} + \underline{\text{c}}_{h,t}\underline{\text{r}}_{h,t}\Big)\Bigg) \quad (1)$$

The objective function to be minimized (1) is composed by two general terms: (i) the operating cost function $\mathscr{C}_i^G(\cdot)$, start-up ($\boldsymbol{c}_i^{\text{SU}}$) and shutdown ($\boldsymbol{c}_i^{\text{SD}}$) costs, and up/down reserve scheduling costs, with reserve costs given by $\boldsymbol{c}_i^{\text{UP}}$ and $\boldsymbol{c}_i^{\text{DW}}$, respectively, for each thermal unit $i \in \mathcal{I}$ along each operating hour $t \in \mathcal{T}$; and (ii) the cost of storing and producing energy from the BESS units $\mathscr{C}_h^S(\cdot)$ and the cost of scheduling up/down reserves, with (revealed) marginals given by $\overline{\text{c}}_h$ and $\underline{\text{c}}_h$, for each storage unit in the system $h \in \mathcal{H}$ along each operating hour $t \in \mathcal{T}$.

3.1.2. Nodal balance and power flow

$$\sum_{i\in\mathcal{I}_n} p_{i,t} + \sum_{l\in\mathcal{L}\,|\,to(l)=n} f_{l,t} - \sum_{l\in\mathcal{L}\,|\,fr(l)=n} f_{l,t} = \hat{d}_{n,t} - \hat{g}_{n,t} + \sum_{h\in\mathcal{H}_n}(\overline{z}_{h,t} - \underline{z}_{h,t});\ \ \forall\ n\in\mathcal{N},\ t\in\mathcal{T} \quad (2)$$

$$f_{l,t} = B_l\Big(\theta_{fr(l),t} - \theta_{to(l),t}\Big); \qquad \forall\ l \in \mathcal{L},\ t \in \mathcal{T} \tag{3}$$

$$-\overline{F}_l \leq f_{l,t} \leq \overline{F}_l; \qquad \forall\ l \in \mathcal{L},\ t \in \mathcal{T}. \tag{4}$$

To model the process of energy delivery through the network, we follow the standard practices with a lossless linear DC representation of the network system as in constraints (2)–(4) [25, 27]. In (2), $\hat{d}_{n,t}$ and $\hat{g}_{n,t}$ represent the nominal demand and vRES output, respectively, at each bus $n \in \mathcal{N}$ of the system and operating hour $t \in \mathcal{T}$, in (3), B_l stands for the susceptance of the transmission line $l \in \mathcal{L}$, whereas $\overline{F}_l$ in (4) indicates the corresponding transmission line capacity.

3.1.3. Generators

$$\underline{P}_i u_{i,t} + r^{\mathrm{DW}}_{i,t} \leq p_{i,t} \leq \overline{P}_i u_{i,t} - r^{\mathrm{UP}}_{i,t}; \qquad \forall\ i \in \mathcal{I},\ t \in \mathcal{T} \tag{5}$$

$$0 \leq r^{\mathrm{UP}}_{i,t} \leq \overline{R}^{\mathrm{UP}}_i u_{i,t}; \qquad \forall\ i \in \mathcal{I},\ t \in \mathcal{T} \tag{6}$$

$$0 \leq r^{\mathrm{DW}}_{i,t} \leq \overline{R}^{\mathrm{DW}}_i u_{i,t}; \qquad \forall\ i \in \mathcal{I},\ t \in \mathcal{T} \tag{7}$$

$$p_{i,t} - p_{i,t-1} \leq \mathrm{RU}_i u_{i,t-1} + \mathrm{SU}_i(u_{i,t} - u_{i,t-1}) + \overline{P}_i(1 - u_{i,t}); \forall\ i \in \mathcal{I},\ t \in \mathcal{T} \tag{8}$$

$$p_{i,t-1} - p_{i,t} \leq \mathrm{RD}_i u_{i,t} + \mathrm{SD}_i(u_{i,t-1} - u_{i,t}) + \overline{P}_i(1 - u_{i,t-1}); \forall\ i \in \mathcal{I},\ t \in \mathcal{T} \tag{9}$$

$$\big(\boldsymbol{c}^{\mathrm{SU}}_i, \boldsymbol{c}^{\mathrm{SD}}_i, \boldsymbol{u}_i\big) \in \mathcal{U}_i; \qquad \forall\ i \in \mathcal{I}. \tag{10}$$

The set of constraints (5)–(10) is adapted from [32] to include reserves. Essentially, expressions (5)–(10) model the feasible region of the thermal generation units. In (5), the power and reserves scheduling capacity of each thermal unit $i \in \mathcal{I}$ are bounded by its inflexibility level ($\underline{P}_i$) and maximum available power ($\overline{P}_i$), (6)–(7) bounds the up/down reserve scheduling to $\overline{R}^{\mathrm{UP}}_i$ and $\overline{R}^{\mathrm{DW}}_i$, respectively, constraints (8)–(9) model the up and down ramping limits (RU_i and RD_i) along with the minimum ramp rate levels of start-up (SU_i) and shutdown (SD_i), and, finally, constraints (10) map the startup/shutdown costs and minimum up and down time constraints of thermal units, with $\mathcal{U}_i$ thoroughly described in Appendix A.

3.1.4. Storage systems

$$v_{ht} = v_{h,t-1} + \overline{\eta}_h \overline{z}_{h,t} - \frac{\underline{z}_{h,t}}{\underline{\eta}_h}; \qquad \forall\ h \in \mathcal{H},\ t \in \mathcal{T} \tag{11}$$

$$\underline{V}_h \leq v_{h,t} \leq \overline{V}_h; \qquad \forall\ h \in \mathcal{H},\ t \in \mathcal{T} \cup \{0\} \tag{12}$$

$$\overline{Z}^{\min}_h \leq \overline{z}_{h,t} + \overline{\mathrm{r}}_{h,t} \leq \overline{Z}^{\max}_h; \qquad \forall\ h \in \mathcal{H},\ t \in \mathcal{T} \tag{13}$$

$$\underline{Z}^{\min}_h \leq \underline{z}_{h,t} + \underline{\mathrm{r}}_{h,t} \leq \underline{Z}^{\max}_h; \qquad \forall\ h \in \mathcal{H},\ t \in \mathcal{T} \tag{14}$$

$$v_{h,|\mathcal{T}|} = v_{h,0}; \qquad \forall\ h \in \mathcal{H}. \tag{15}$$

As usually modeled in the technical literature (see [10] for example), constraints (11)–(15) outline the feasible region of BESSs. More specifically, (11) recover the energy storage time coupling with $\overline{\eta}_h$ and $\underline{\eta}_h$ representing, respectively, the efficiency rate to store and produce energy of storage unit $h \in \mathcal{H}$ with (12) imposing the physical upper ($\overline{V}_h$) and lower ($\underline{V}_h$) bounds for the energy storage level of unit $h \in \mathcal{H}$ at the end of hour $t \in \mathcal{T}$. Constraints (13) and (14) characterize the minimum and maximum limits of power storage (withdrawal from the system) and production (injection into the system) of each storage system $h \in \mathcal{H}$, with $\overline{Z}_h^{\min}$ and $\overline{Z}_h^{\max}$ indicating the bounds for the withdraws and, similarly, $\underline{Z}_h^{\min}$ and $\underline{Z}_h^{\max}$ standing for the bounds for injection. Finally, (15) impose the state of charge of each storage device $h \in \mathcal{H}$ at the end of the operating period to be equivalent to its initial value.

3.1.5. Risk constraint

$$\text{CVaR}_{\alpha}\Big(\mathscr{L}_t\big(\mathbf{x}^G, \mathbf{x}^S, \tilde{\boldsymbol{g}}\big)\Big) \leq \overline{\mathscr{L}}_t; \qquad \forall\, t \in \mathcal{T}. \tag{16}$$

As previously discussed, two of the most critical uncertainties in power system operations are the variability of vRES output (which can be characterized by a collection of exogenous scenarios) and uncertainty in equipment availability (which can be modeled by means of an exogenously-defined set of credible contingency states) in the real-time energy delivery stage. In this work, we directly tackle these uncertainties in operations by restricting the CVaR of the total system imbalance distribution to an *a-priori* user-defined tolerance level $\overline{\mathscr{L}}_t$ at each hour of the operating stage $t \in \mathcal{T}$ as in (16). In this constraint, $\mathscr{L}_t(\cdot)$ is a functional that recovers the worst-case contingency-adjusted real-time system imbalance level at a given hour of the operating stage $t \in \mathcal{T}$ for an operating point defined by power and reserves scheduling of conventional generators ($\mathbf{x}^G$) and storage systems ($\mathbf{x}^S$), and a random-vector of renewable energy production ($\tilde{\boldsymbol{g}}$). In the next subsection, we formally describe the functional $\big\{\mathscr{L}_t(\cdot)\big\}_{t\in\mathcal{T}}$ along with the structure of the operating stage.

3.2. Least Worst-Case Contingency-Adjusted System Imbalance Assessment Problem

Once the uncertainty realization is revealed, the system can be redispatched with the available resources (determined during the day-ahead operation planning) in a decision-making process that can be formulated as an optimization problem. Formally, let Ω denote a finite set of vRES output $\big\{\boldsymbol{g}_\omega\big\}_{\omega\in\Omega}$ with probability measure $\boldsymbol{\rho} \triangleq \big\{\rho_\omega\big\}_{\omega\in\Omega}$ over Ω, and $\boldsymbol{a} \triangleq \big\{\{a^G_{i,t}\}_{i\in\mathcal{I}}, \{a^L_{l,t}\}_{l\in\mathcal{L}}\big\}_{t\in\mathcal{T}}$ a vector of the availability statuses of transmission assets $\big(\boldsymbol{a}^L \triangleq \{a^L_{l,t}\}_{l\in\mathcal{L},t\in\mathcal{T}}\big)$ and conventional generation units $\big(\boldsymbol{a}^G \triangleq \{a^G_{i,t}\}_{i\in\mathcal{I},t\in\mathcal{T}}\big)$. Then, for a given power and reserves scheduling of conventional generators ($\mathbf{x}^G$) and storage systems ($\mathbf{x}^S$), the contingency-aware economic re-dispatch problem is given by (17)–(30).

$$\Delta\big(\mathbf{x}^G, \mathbf{x}^S, \boldsymbol{g}_\omega, \boldsymbol{a}\big) = \min_{\substack{\boldsymbol{p}^{(\boldsymbol{a})}_\omega, \boldsymbol{f}^{(\boldsymbol{a})}_\omega, \boldsymbol{\theta}^{(\boldsymbol{a})}_\omega, \\ \boldsymbol{v}^{(\boldsymbol{a})}_\omega, \overline{\boldsymbol{z}}^{(\boldsymbol{a})}_\omega, \underline{\boldsymbol{z}}^{(\boldsymbol{a})}_\omega \\ \overline{\boldsymbol{\delta}}^{(\boldsymbol{a})}_\omega, \underline{\boldsymbol{\delta}}^{(\boldsymbol{a})}_\omega}} \; \sum_{t\in\mathcal{T}}\sum_{n\in\mathcal{N}} \Big(\overline{\delta}^{(\boldsymbol{a})}_{n,t,\omega} + \underline{\delta}^{(\boldsymbol{a})}_{n,t,\omega}\Big) \tag{17}$$

subject to:

$$\sum_{i\in\mathcal{I}_n} p^{(\boldsymbol{a})}_{i,t,\omega} + \sum_{l\in\mathcal{L}\mid to(l)=n} f^{(\boldsymbol{a})}_{l,t,\omega} - \sum_{l\in\mathcal{L}\mid fr(l)=n} f^{(\boldsymbol{a})}_{l,t,\omega} = \hat{d}_{n,t} - g_{n,t,\omega} + \sum_{h\in\mathcal{H}_b}\left(\overline{z}^{(\boldsymbol{a})}_{h,t,\omega} - \underline{z}^{(\boldsymbol{a})}_{h,t,\omega}\right) + \overline{\delta}^{(\boldsymbol{a})}_{n,t,\omega} - \underline{\delta}^{(\boldsymbol{a})}_{n,t,\omega}; \qquad \forall\, n\in\mathcal{N},\ t\in\mathcal{T} \quad (18)$$

$$f^{(\boldsymbol{a})}_{l,t,\omega} = a^L_{l,t} B_l\Big(\theta^{(\boldsymbol{a})}_{fr(l),t,\omega} - \theta^{(\boldsymbol{a})}_{to(l),t,\omega}\Big); \qquad \forall\, l\in\mathcal{L},\ t\in\mathcal{T} \quad (19)$$

$$-\overline{F}_l \le f^{(\boldsymbol{a})}_{l,t,\omega} \le \overline{F}_l; \qquad \forall\, l\in\mathcal{L},\ t\in\mathcal{T} \quad (20)$$

$$a^G_{i,t}\big(p_{i,t} - r^{\mathrm{DW}}_{i,t}\big) \le p^{(\boldsymbol{a})}_{i,t,\omega} \le a^G_{i,t}\big(p_{i,t} + r^{\mathrm{UP}}_{i,t}\big); \qquad \forall\, i\in\mathcal{I},\ t\in\mathcal{T} \quad (21)$$

$$p^{(\boldsymbol{a})}_{i,t,\omega} - p^{(\boldsymbol{a})}_{i,t-1,\omega} \le \mathrm{RU}_i; \qquad \forall\, i\in\mathcal{I},\ t\in\mathcal{T} \quad (22)$$

$$p^{(\boldsymbol{a})}_{i,t-1,\omega} - p^{(\boldsymbol{a})}_{i,t,\omega} \le \mathrm{RD}_i; \qquad \forall\, i\in\mathcal{I},\ t\in\mathcal{T} \quad (23)$$

$$v^{(\boldsymbol{a})}_{h,t,\omega} = v^{(\boldsymbol{a})}_{h,t-1,\omega} + \overline{\eta}_h \overline{z}^{(\boldsymbol{a})}_{h,t,\omega} - \frac{\underline{z}^{(\boldsymbol{a})}_{h,t,\omega}}{\underline{\eta}_h}; \qquad \forall\, h\in\mathcal{H},\ t\in\mathcal{T} \quad (24)$$

$$\underline{V}_h \le v^{(\boldsymbol{a})}_{h,t,\omega} \le \overline{V}_h; \qquad \forall\, h\in\mathcal{H},\ t\in\mathcal{T}\cup\{0\} \quad (25)$$

$$\overline{z}_{h,t} \le \overline{z}^{(\boldsymbol{a})}_{h,t,\omega} \le \overline{z}_{h,t} + \overline{\mathrm{r}}_{h,t}; \qquad \forall\, h\in\mathcal{H},\ t\in\mathcal{T} \quad (26)$$

$$\underline{z}_{h,t} \le \underline{z}^{(\boldsymbol{a})}_{h,t,\omega} \le \underline{z}_{h,t} + \underline{\mathrm{r}}_{h,t}; \qquad \forall\, h\in\mathcal{H},\ t\in\mathcal{T} \quad (27)$$

$$v^{(\boldsymbol{a})}_{h,0,\omega} = v_{h,0}; \qquad \forall\, h\in\mathcal{H} \quad (28)$$

$$v^{(\boldsymbol{a})}_{h,|\mathcal{T}|,\omega} = v_{h,0}; \qquad \forall\, h\in\mathcal{H} \quad (29)$$

$$\overline{\delta}^{(\boldsymbol{a})}_{n,t,\omega}, \underline{\delta}^{(\boldsymbol{a})}_{n,t,\omega} \ge 0; \qquad \forall\, n\in\mathcal{N},\ t\in\mathcal{T}. \quad (30)$$

Problem (17)–(30) falls into the class of linear and continuous optimization problems and seeks to minimize the (positive and negative) system-wide imbalance, as in equation (17), using the power and reserves from the day-ahead schedule $\big(\mathbf{x}^G, \mathbf{x}^S\big)$, given an uncertain factor $\big(\boldsymbol{g}_\omega, \boldsymbol{a}\big)$ realization, as a second-stage (recourse) solution. It has a similar structure as problem (1)–(16). More specifically, the block of constraints (18)–(20) models the process of energy delivery through the network with $a^L_{l,t}$ in (19) indicating the status of the transmission line $l\in\mathcal{L}$ in hour $t\in\mathcal{T}$. Furthermore, the block of constraints (21)–(23) define the feasible re-dispatch region of each thermal generator unit $i\in\mathcal{I}$ in $t\in\mathcal{T}$. Note that the day-ahead thermal scheduling is explicitly taken into account in (21) with $a^G_{i,t}$ indicating the status of the unit $i\in\mathcal{I}$ along $t\in\mathcal{T}$. Similarly, the block of constraints (24)–(29) stand for the feasible operating region of the BESSs, with their day-ahead scheduling explicitly taken into account in (26)–(27). Finally, (30) states the bounds for the positive $\big(\overline{\delta}^{(\boldsymbol{a})}_{n,t,\omega}\big)$ and negative $\big(\underline{\delta}^{(\boldsymbol{a})}_{n,t,\omega}\big)$ system imbalance at each bus $n\in\mathcal{N}$ and operating hour $t\in\mathcal{T}$.

To tackle the uncertainty in the availability of system assets during the actual energy delivery stage, we follow the standard industry practice, namely, the definition of an *a priori* set of credible contingency states $\mathcal{A}$. Formally, this process can be stated as in (31).

$$\boldsymbol{a}^*_\omega \in \arg\max_{\boldsymbol{a}} \Big\{\Delta\big(\mathbf{x}^G, \mathbf{x}^S, \boldsymbol{g}_\omega, \boldsymbol{a}\big) \;\Big|\; \boldsymbol{a}\in\mathcal{A}\Big\}. \quad (31)$$

Finally, for a given planning of power and reserves scheduling of conventional generators ($\mathbf{x}^G$) and storage systems ($\mathbf{x}^S$), and a renewable generation output $\boldsymbol{g}_\omega$, the contingency-adjusted system-wide imbalance functional $\mathscr{L}_t(\cdot)$ in each hour $t \in \mathcal{T}$ can be, thus, computed as follows:

$$\mathscr{L}_t\big(\mathbf{x}^G, \mathbf{x}^S, \boldsymbol{g}_\omega\big) = \sum_{n \in \mathcal{N}} \Big(\overline{\delta}_{n,t,\omega}^{(\boldsymbol{a}_\omega^*)} + \underline{\delta}_{n,t,\omega}^{(\boldsymbol{a}_\omega^*)} \Big). \tag{32}$$

In should be noted that, following its mathematical structure, the day-ahead scheduling process is a particular instance of a three-level system of mathematical programming models that cannot be solved by standard optimization techniques. Therefore, to overcome this challenge, in the next section, a reformulation procedure is designed to transform the non-tractable day-ahead scheduling problem (1)–(16) into a semi-infinte optimization model and, then, an efficient solution approach based on Column-and-Constraint Generation (CCG) techniques is devised to handle the resulting problem.

4. Solution Methodology

In order to computationally solve the three-level system of mathematical programming models presented in Section 3, an efficient solution methodology is minutely described in this section. We begin by reducing the tri-level structure (1)–(16) into an equivalent single-level, semi-infinite optimization problem (Subsection 4.1) by leveraging the dual representation of the CVaR_α functional. Afterward, a tailored Column-and-Constraint Generation (CCG) algorithm is designed in Subsection 4.2 to efficiently solve the resulting optimization problem.

4.1. Single-Level Equivalent Formulation

The main challenge to solve the optimization problem (1)–(16) is to handle the set of constraints (16) since optimization models are involved in their left-hand side. Our first step towards developing a tractable solution methodology is to reformulate (1)–(16) into an equivalent single model that does not have any intrinsic optimization model within any of its constraints. In the following proposition, we state this reformulation can be done and prove it.

Proposition 1. *The multilevel optimization problem* (1)–(16) *can be reformulated into a single-level equivalent formulation.*

Proof. To begin with, without loss of generality, problem (1)–(16) can be written in compact form as:

$$\underset{\substack{\mathbf{x}^G,\boldsymbol{u},\boldsymbol{c}^{\mathrm{SU}},\boldsymbol{c}^{\mathrm{SD}},\mathbf{x}^S,\\ \boldsymbol{f},\boldsymbol{\theta},\mathbf{y}}}{\text{Minimize}} \quad \mathscr{C}\Big(\mathbf{x}^G,\boldsymbol{u},\boldsymbol{c}^{\mathrm{SU}},\boldsymbol{c}^{\mathrm{SD}},\mathbf{x}^S\Big) \tag{33}$$

subject to:

$$\Big(\mathbf{x}^G,\boldsymbol{u},\mathbf{x}^S,\boldsymbol{f},\boldsymbol{\theta},\boldsymbol{c}^{\mathrm{SU}},\boldsymbol{c}^{\mathrm{SD}}\Big) \in \mathcal{X}; \tag{34}$$

$$\mathrm{CVaR}_\alpha\Big(\mathscr{L}_t\big(\mathbf{x}^G,\mathbf{x}^S,\tilde{\boldsymbol{g}}\big)\Big) \leq \overline{\mathscr{L}}_t; \qquad \forall\, t \in \mathcal{T}., \tag{35}$$

where, function $\mathscr{C}(\cdot)$ maps the objective function (1) and $\mathcal{X}$ comprises the set of constraints (2)–(15). For a given operating point $(\mathbf{x}^G,\mathbf{x}^S)$ and scenario $\omega \in \Omega$ of vRES output, let $\boldsymbol{a}^*_\omega$ be the contingency state with the highest system imbalance, i.e., a solution for the optimization problem (31), which is presented next in its compact form in (36).

$$\boldsymbol{a}^*_\omega \in \underset{\boldsymbol{a}\in\mathcal{A}}{\arg\max} \left\{ \min_{\mathbf{y}^{(\boldsymbol{a})}_\omega} \sum_{t\in\mathcal{T}} \boldsymbol{e}_t^\top \mathbf{y}^{(\boldsymbol{a})}_{t,\omega} \right.$$
$$\text{subject to:}$$
$$\left. \Big\{\mathbf{y}^{(\boldsymbol{a})}_{t,\omega}\Big\}_{t\in\mathcal{T}} \in \mathcal{Y}\big(\mathbf{x}^G,\mathbf{x}^S,\boldsymbol{g}_\omega,\boldsymbol{a}\big) \right\}, \tag{36}$$

In (36), $\boldsymbol{e}_t$ recovers the linear objective function (17) for each $t \in \mathcal{T}$. Also in (36), $\{\mathbf{y}^{(\boldsymbol{a})}_{t,\omega}\}_{t\in\mathcal{T}}$ and $\mathcal{Y}\big(\mathbf{x}^G,\mathbf{x}^S,\boldsymbol{g}_\omega,\boldsymbol{a}\big)$ denote, respectively, the vector of decision variables and feasible region (18)–(30) of the re-dispatch problem. In this context, for each time period $t \in \mathcal{T}$, the imbalance function $\mathscr{L}_t(\mathbf{x}^G,\mathbf{x}^S,\boldsymbol{g}_\omega)$ in (16), can be properly evaluated by setting:

$$\mathscr{L}_t\big(\mathbf{x}^G,\mathbf{x}^S,\boldsymbol{g}_\omega\big) = \boldsymbol{e}_t^\top \mathbf{y}^{(\boldsymbol{a}^*)}_{t,\omega}, \tag{37}$$

following (32). Therefore, by making use of the dual representation of the CVaR_α risk measure [12], a sufficient condition for the block of constraints (16) to hold is:

$$\overline{\mathscr{L}}_t \geq \mathrm{CVaR}_\alpha\Big(\mathscr{L}_t\big(\mathbf{x}^G,\mathbf{x}^S,\tilde{\boldsymbol{g}}\big)\Big) \tag{38}$$

$$= \max_{\boldsymbol{q}_t\in\mathcal{Q}_\alpha(\boldsymbol{\rho})} \left\{ \sum_{\omega\in\Omega} q_{t,\omega}\Big(\boldsymbol{e}_t^\top \mathbf{y}^{(\boldsymbol{a}^*)}_{t,\omega}\Big) \right\} \tag{39}$$

$$\geq \sum_{\omega\in\Omega} q_{t,\omega}\Big(\boldsymbol{e}_t^\top \mathbf{y}^{(\boldsymbol{a}^*)}_{t,\omega}\Big), \qquad \forall\, \boldsymbol{q}_t \in \mathcal{Q}_\alpha(\boldsymbol{\rho}),\ t \in \mathcal{T} \tag{40}$$

with

$$\mathcal{Q}_\alpha(\boldsymbol{\rho}) = \left\{ \boldsymbol{q} \in \mathbb{R}^{|\Omega|} \;\middle|\; \begin{array}{l} \displaystyle\sum_{\omega\in\Omega} q_\omega = 1; \\ \\ 0 \leq q_\omega \leq \rho_\omega/(1-\alpha), \quad \omega \in \Omega; \end{array} \right\}$$

and $\rho_\omega = \mathbb{P}(\{\omega\})$ the probability measure of scenario $\omega \in \Omega$.

Hence, the power and reserves scheduling problem of the conventional and storage units (1)–(16) can be equivalently re-written as the single-level optimization model (41)–(44).

$$\underset{\substack{\mathbf{x}^G,\boldsymbol{u},\boldsymbol{c}^{\mathrm{SU}},\boldsymbol{c}^{\mathrm{SD}},\mathbf{x}^S,\\ \boldsymbol{f},\boldsymbol{\theta},\mathbf{y}}}{\text{Minimize}} \; \mathscr{C}\left(\mathbf{x}^G,\boldsymbol{u},\boldsymbol{c}^{\mathrm{SU}},\boldsymbol{c}^{\mathrm{SD}},\mathbf{x}^S\right) \tag{41}$$

subject to:

$$\left(\mathbf{x}^G,\boldsymbol{u},\mathbf{x}^S,\boldsymbol{f},\boldsymbol{\theta},\boldsymbol{c}^{\mathrm{SU}},\boldsymbol{c}^{\mathrm{SD}}\right) \in \mathcal{X}; \tag{42}$$

$$\sum_{\omega\in\Omega} q_{t,\omega}\left(\boldsymbol{e}_t^\top \mathbf{y}_{t,\omega}^{(\boldsymbol{a})}\right) \leq \overline{\mathscr{L}}_t; \qquad \forall\, \boldsymbol{q}_t \in \mathcal{Q}_\alpha(\boldsymbol{\rho}),\ t \in \mathcal{T},\ \boldsymbol{a} \in \mathcal{A} \tag{43}$$

$$\left\{\mathbf{y}_{t,\omega}^{(\boldsymbol{a})}\right\}_{t\in\mathcal{T}} \in \mathcal{Y}\left(\mathbf{x}^G,\mathbf{x}^S,\boldsymbol{g}_\omega,\boldsymbol{a}\right). \qquad \forall\, \omega \in \Omega,\ \boldsymbol{a} \in \mathcal{A} \tag{44}$$

■

However, even though we managed to prove that the multi-level optimization problem (1)–(16) can be equivalently rewritten as the single level optimization problem (41)–(44), it is still computationally intractable to solve (41)–(44) in its current form. Essentially, problem (41)–(44) fits within the class of a semi-infinite mixed-integer programming problem [33], recognized as hard to be solved by standard mathematical programming techniques in a suitable computational time. Therefore, in the next section, the CCG technique is adapted to (41)–(44) aiming at designing a computationally efficient solution procedure for the proposed power and reserve scheduling problem (1)–(16).

4.2. Column-and-Constraint Generation Algorithm

The goal of this section is to design an efficient solution procedure for the semi-infinite mixed-integer programming problem (41)–(44) by adapting the column-and-constraint generation technique. Roughly speaking, the CCG algorithmic framework is a computational procedure within the class of master\oracle-decomposition algorithms that aims to iteratively assess the most critical structural blocks of a large-scale optimization problem that are sufficient to characterize an optimality subset of the problem [13, 34, 35]. In the particular context of this work, we set up (i) a master problem that is a relaxed version of (41)–(44), where the full set of contingency states $\mathcal{A}$ is replaced by $\hat{\mathcal{A}} \subset \mathcal{A}$ and the full collection of sets of probability measures $\mathcal{Q}_\alpha(\boldsymbol{\rho})$ is replaced by $\left\{\hat{\mathcal{Q}}_t\right\}_{t\in\mathcal{T}} \subset \mathcal{Q}_\alpha(\boldsymbol{\rho})$ and (ii) a oracle problem that identifies contingency states to be included in $\hat{\mathcal{A}}$ and probability measures to be included in $\left\{\hat{\mathcal{Q}}_t\right\}_{t\in\mathcal{T}}$ at every iteration to improve the solution of the master problem. In the execution of our proposed algorithm, sets $\hat{\mathcal{A}}$ and $\left\{\hat{\mathcal{Q}}_t\right\}_{t\in\mathcal{T}}$ begin in

the master problem with any small subset of $\mathcal{A}$ and $\mathcal{Q}_\alpha(\boldsymbol{\rho})$, respectively, that contains at least one element at first and are iteratively provided with elements until they obtain information to make the solution of the master problem optimal for (41)–(44). The proposed CCG algorithm is described in Algorithm 1.

Algorithm 1 – Column-and-Constraint Generation Algorithm

Initialization:

Set $m \leftarrow 1$.

Choose an initial subset of contingency states $\hat{\mathcal{A}}^{(1)} \subset \mathcal{A}$ and a collection of sets $\{\hat{\mathcal{Q}}_t^{(1)}\}_{t\in\mathcal{T}} \subset \mathcal{Q}_\alpha(\boldsymbol{\rho})$.

Iteration $m \geq 1$:

Step 1 – ***Master Problem***: Identify a power and reserves scheduling for conventional and storage units $(\mathbf{x}_G^{(m)}, \mathbf{x}_S^{(m)})$ by solving the MILP problem (41)–(44) with $\hat{\mathcal{A}}^{(m)}$ and the collection $\{\hat{\mathcal{Q}}_t^{(m)}\}_{t\in\mathcal{T}}$ in (43)–(44).

Step 2 – ***Oracle***: For all $\omega \in \Omega$, solve problem (36) with $(\mathbf{x}_G^{(m)}, \mathbf{x}_S^{(m)})$, and collect its solution vector $\boldsymbol{a}_\omega^*$. Then, for each time period $t \in \mathcal{T}$, compute the $\text{CVaR}_\alpha\big(\mathscr{L}_t(\mathbf{x}_G^{(m)}, \mathbf{x}_S^{(m)}, \tilde{\boldsymbol{g}})\big)$ by using (37) and (39), and store its optimal vector $\{\boldsymbol{q}_t^*\}_{t\in\mathcal{T}}$.

if $\exists\, t \in \mathcal{T} \mid \text{CVaR}_\alpha\big(\mathscr{L}_t(\mathbf{x}_G^{(m)}, \mathbf{x}_S^{(m)}, \tilde{\boldsymbol{g}})\big) > \overline{\mathscr{L}}_t$

Update $\hat{\mathcal{A}}^{(m+1)} \leftarrow \hat{\mathcal{A}}^{(m)} \cup \{\boldsymbol{a}_\omega^*\}_{\omega\in\Omega}$ and the sets $\hat{\mathcal{Q}}_t^{(m+1)} \leftarrow \hat{\mathcal{Q}}_t^{(m)} \cup \{\boldsymbol{q}_t^*\},\ \forall\, t \in \mathcal{T}$.

Set $m \leftarrow m + 1$.

else

Return $(\mathbf{x}_G^{(m)}, \mathbf{x}_S^{(m)})$.

end if

In **Step 2** of Algorithm 1, the problem formulated as the two-level system of mathematical programming models (36) needs to be solved at each iteration m in order to obtain the contingency vector $\boldsymbol{a}_\omega^*$ for each scenario $\omega \in \Omega$. However, this problem cannot be directly solved using standard mathematical programming algorithms. Nevertheless, by leveraging the linear and continuous structure of the inner problem, we can re-write the bilevel optimization problem as an equivalent single-level counterpart with the following three steps [36].

1. Derive the dual problem of (17)–(30).
2. In (36), co-optimize the outer problem with the dual of the inner problem as a single maximization model.
3. Reformulate the bilinear terms of continuous and binary variables using an exact relaxation following McCormick envelopes [37].

Proposition 2. *Algorithm 1 terminates in a finite number of steps and provides the optimal solution to problem* (41)–(44).

Proof. At the first iteration of Algorithm 1, the iteration counter m is set equal to 1 and the initial small subset $\hat{\mathcal{A}}^{(1)} \subset \mathcal{A}$ contains any single element of $\mathcal{A}$ composed of a vector $\boldsymbol{a}_\omega$ for each $\omega in \Omega$. In addition, each set of the initial collection of sets $\{\hat{\mathcal{Q}}_t^{(1)}\}_{t\in\mathcal{T}} \subset \mathcal{Q}_\alpha(\boldsymbol{\rho})$ contains any single vector $\boldsymbol{q}_t \subset \mathcal{Q}_\alpha(\boldsymbol{\rho})$. So, by

replacing $\mathcal{A}$ with $\hat{\mathcal{A}}^{(1)}$ and $\mathcal{Q}_\alpha(\boldsymbol{\rho})$ with $\left\{\hat{\mathcal{Q}}_t^{(1)}\right\}_{t\in\mathcal{T}}$ in problem (41)–(44), we obtain our master problem, which is essentially a relaxed version of (41)–(44).

Let the full uncertainty set be a cartesian product of $\mathcal{A}$ and $\mathcal{Q}_\alpha(\boldsymbol{\rho})$ written as follows.

$$\Phi = \Bigg\{ \{\boldsymbol{a}_\omega \in \{0,1\}^{(|I|+|\mathcal{L}|)}\}_{\omega\in\Omega}, \{\boldsymbol{q}_t \in \mathbb{R}^{|\Omega|}\}_{t\in\mathcal{T}} \Bigg| \begin{aligned} & \boldsymbol{W}\boldsymbol{a}_\omega \geq \mathbf{w}; \forall \omega \in \Omega \\ & \sum_{\omega\in\Omega} q_\omega = 1; \forall t \in \mathcal{T} \\ & 0 \leq q_\omega \leq \rho_\omega/(1-\alpha); \forall \omega \in \Omega, t \in \mathcal{T} \Bigg\}, \end{aligned} \tag{45}$$

where matrix $\boldsymbol{W}$ and vector $\mathbf{w}$ contain user-defined elements that belong to $\mathbb{R}$. The uncertainty set Φ has an infinite number of elements and that is why problem (41)–(44) is a semi-infinite mixed-integer programming problem. Nonetheless, since Φ is a polyhedral uncertainty set, we only need to include in $\hat{\mathcal{A}}^{(m)}$ and $\left\{\hat{\mathcal{Q}}_t^{(m)}\right\}_{t\in\mathcal{T}}$ the elements $\{\boldsymbol{a}_\omega \in \{0,1\}^{(|I|+|\mathcal{L}|)}\}_{\omega\in\Omega}$ and $\{\boldsymbol{q}_t \in \mathbb{R}^{|\Omega|}\}_{t\in\mathcal{T}}$, respectively, that correspond to the vertexes of the feasible region defined by Φ to make the solution of the master problem optimal to the problem (41)–(44).

At each iteration m, given an operating point $(\mathbf{x}^G, \mathbf{x}^S)$ provided by the incumbent master problem solution, the algorithm solves problem (36) to obtain an element $\{\boldsymbol{a}_\omega \in \{0,1\}^{(|I|+|\mathcal{L}|)}\}_{\omega\in\Omega}$ and problem (39) to obtain an element $\{\boldsymbol{q}_t \in \mathbb{R}^{|\Omega|}\}_{t\in\mathcal{T}}$. This pair of elements $\{\boldsymbol{a}_\omega \in \{0,1\}^{(|I|+|\mathcal{L}|)}\}_{\omega\in\Omega}$ and $\{\boldsymbol{q}_t \in \mathbb{R}^{|\Omega|}\}_{t\in\mathcal{T}}$ constitutes a vertex to the feasible region of the uncertainty set Φ and is used to update $\hat{\mathcal{A}}^{(m)}$ and $\left\{\hat{\mathcal{Q}}_t^{(m)}\right\}_{t\in\mathcal{T}}$, respectively, in the master problem.

Therefore, Algorithm 1 will provide the optimal solution to the problem (41)–(44) in a finite number of steps because it will either (i) include all the finite number vertexes of the uncertainty set Φ in the master problem or (ii) the subset of vertexes of the uncertainty set Φ whose corresponding constraints are active in the optimal solution of the master problem. The algorithm notices that no other vertex of the uncertainty set is needed to be included in the master problem when the optimal objective function value of the problem (39) is lower than the user-defined threshold $\overline{\mathscr{L}}_t$ for all $t \in \mathcal{T}$, which essentially means that none non-included vertex can provide the master problem with information that would violate constraint (43).

■

Remark. *Note that the dual representation of the CVaR$_\alpha$ risk measure* (39) *can be viewed as a constrained knapsack problem [12]. Thus, the solution vector* $\boldsymbol{q}$ *of probability measures is composed by several null values. More specifically, the idea is that the CVaR$_\alpha$ can be interpreted as the average of the* $(1-\alpha)$ *worst-valued scenarios and the vector* $\boldsymbol{q}$ *precisely represents the respective conditional probability to compute such average [12, 38]. Therefore, a significant portion of* $\boldsymbol{q}$ *is set at zero at the optimal solution, representing those scenarios that are not involved in the evaluation of the conditional average. As a consequence, in order to enhance the computational capability of the proposed methodology, in the* ***Step 2*** *of every iteration* m *of the*

CCG algorithm, it is only necessary to store the variables $\{q_{j,\omega}^{(m)}, \boldsymbol{a}_{j,\omega}^{(m)}\}_{\omega\in\Omega, j\in\mathcal{J}}$ *associated with scenarios such that* $q_{j,\omega}^{(m)} > 0$*, thus reducing the size of the Master Problem to be solved in* ***Step 1****.*

Proposition 3. *Algorithm 1 terminates in a finite number of steps and provides the optimal solution to the original problem* (1)–(16)*.*

PROOF. **Proposition 1** states that the original problem (1)–(16) can be equivalently rewritten as problem (41)–(44) and **Proposition 2** states that it is guaranteed that Algorithm 1 provides the optimal solution to problem (41)–(44) in a finite number of steps. Since both **Proposition 1** and **Proposition 2** have been proved, then it is also true that the Algorithm 1 terminates in a finite number of steps and provides the optimal solution to the original problem (1)–(16).

■

5. Case Studies

The performance of the proposed methodology is empirically evaluated in this section with a collection of numerical experiments based on two test systems. The first one is an illustrative 5-bus system, while the second one is based on a simplified representation of the Western Electricity Coordinating Council (WECC) power network [39], hereinafter referred to as `WECC-240`. We consider a credible set of contingency states that follows a contingency-constrained operational setup [40] with uncertainty in the failures of conventional generators, which can be encoded in our methodology by defining $\mathcal{A}$ as in (46).

$$\mathcal{A} = \Bigg\{ \boldsymbol{a} \triangleq \left(\boldsymbol{a}^G, \boldsymbol{a}^L\right) \in \{0,1\}^{|\mathcal{T}|(|\mathcal{L}|+|\mathcal{I}|)} \;\Bigg|\; \begin{aligned} &\sum_{i\in\mathcal{I}} a_{i,1}^G \geq |\mathcal{I}| - K_g; \\ &a_{i,t}^G = a_{i,t-1}^G; && \forall\, t \in \mathcal{T}\setminus\{1\} \\ &\sum_{l\in\mathcal{L}} a_{l,t}^L \geq |\mathcal{L}|; && \forall\, t \in \mathcal{T}; \end{aligned} \Bigg\}. \tag{46}$$

Furthermore, we assume a linear operating cost function for each thermal unit $i \in \mathcal{I}$ and a linear storing and producing energy cost function for each storage system $h \in \mathcal{H}$, i.e.,

$$\mathscr{C}_i^G\left(\boldsymbol{p}_i, \boldsymbol{u}_i\right) = c_{i,t}^{\text{fix}} u_{i,t} + c_{i,t}^{\text{var}} p_{i,t}; \qquad \forall\, i \in \mathcal{I},\ t \in \mathcal{T} \tag{47}$$

$$\mathscr{C}_h^S\left(\boldsymbol{v}_h, \overline{\boldsymbol{z}}_h, \underline{\boldsymbol{z}}_h\right) = c_{h,t}^{\text{ch}} \overline{z}_{h,t} + c_{h,t}^{\text{disc}} \underline{z}_{h,t}; \qquad \forall\, h \in \mathcal{H},\ t \in \mathcal{T}. \tag{48}$$

An Intel® Core i7-10700K 4.8GHz with 64 GB of RAM machine, with Gurobi® Solver 9.0 under JuMP® was used to run all the numerical experiments.

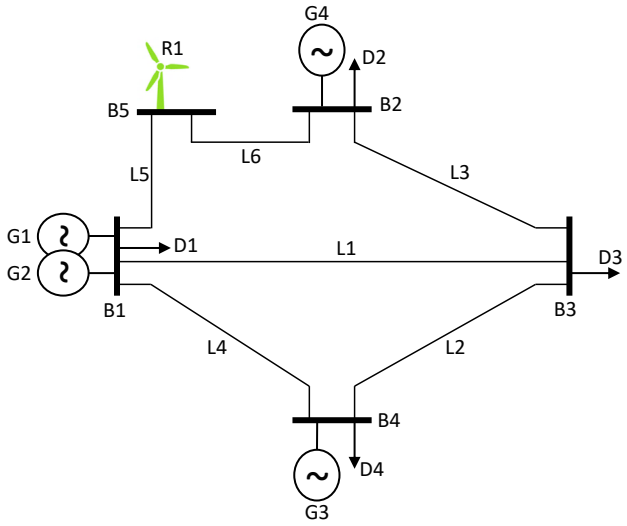

Figure 1: **5-Bus System** – Test system with 5 buses, 6 transmission lines, 4 conventional generators, 1 renewable unit and 1 storage device at bus 5.

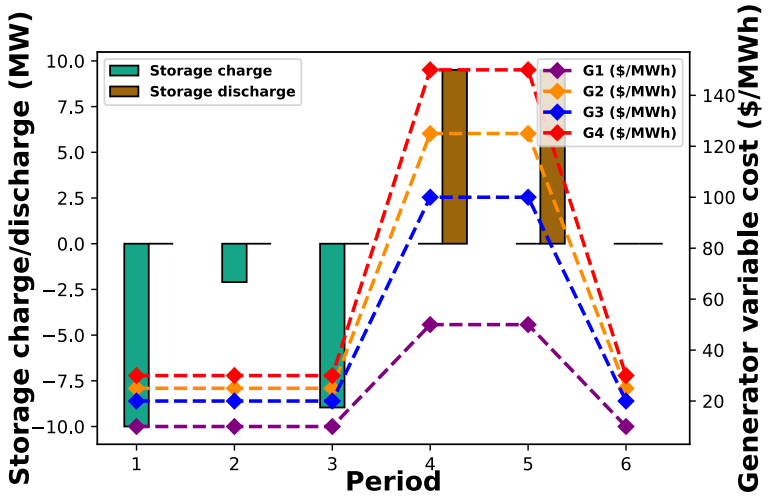

Figure 2: **5-Bus System** – Storage charge and discharge for the case in which storage is considered in the system.

5.1. 5-Bus System

This case study empirically illustrates the benefits of the proposed methodology in a small-scale system (depicted in Fig. 1) that comprises 5 buses, 6 transmission lines, 4 conventional generators and 1 renewable unit. A storage device is placed at bus 5, where the renewable unit is also present. For this 5-bus system, we consider 6 operating time periods, with periods 4 and 5 representing the peak-load, when thermal generation is also more expensive. For comparison purposes, two cases are analyzed: with and without the presence of the storage device in the system. Both scheduling solutions consider a security level represented by imposing $K_g = 1$ in (46) and $\overline{\mathscr{L}}_t$, in (16), are set to 1.5% of the corresponding system-wide demand of each hour. We take into account 100 scenarios of potential realizations of vRES output at bus 5. All data used in this numerical experiment can be found in [41].

In Fig. 2 we depict the charge and discharge of the storage device given by the first scheduling solution

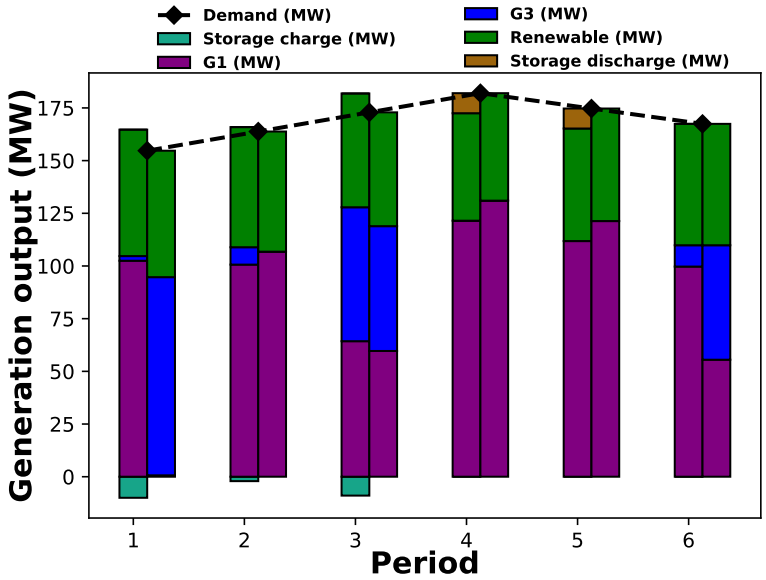

Figure 3: **5-Bus System** – Optimal conventional generation and storage device day-ahead scheduling. For each period, the left bar corresponds to the solution obtained while considering a storage device at bus 5, while the right bar corresponds to the same system without any storage device.

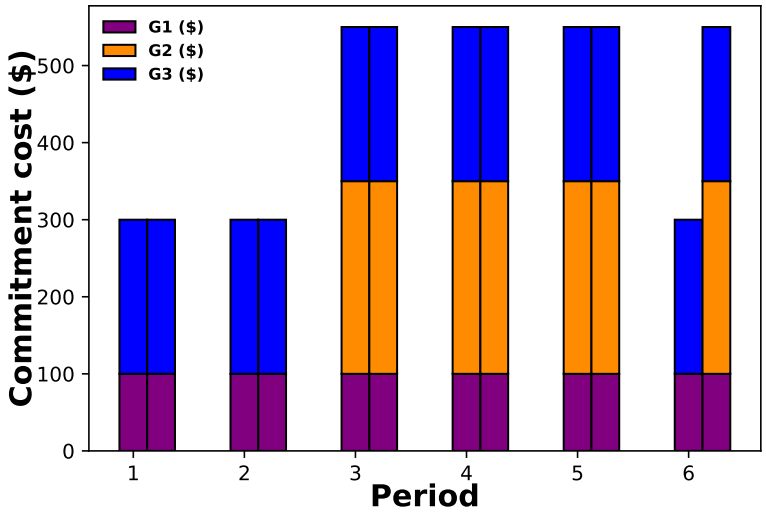

Figure 4: **5-Bus System** – Commitment cost. For each period, the left bar corresponds to the solution obtained while considering a storage device at bus 5, while the right bar corresponds to the same system without any storage device.

and in Fig. 3, we illustrate the conventional generation outputs of the solutions with and without storage. Furthermore, in Fig. 4, the commitment costs for the cases with and without storage are displayed and the comparison of generation ramping with and without storage is provided in Fig. 5 for each scheduling solution. In Fig. 6, required up-spinning reserves with and without storage is compared. Finally, Fig. 7 plots the post-contingency re-dispatch (after the failure of Generator 1 (G1) and the realization of a particular scenario of renewable generation) for the cases with and without storage.

As can be seen in Fig. 2, the storage device basically charged when generation was cheaper and discharged when it was expensive. The effect of this operating profile is also seen in Fig. 3, where the storage discharge decreases the need for expensive conventional generation during peak-hours. Figs. 4–6 demonstrate that the

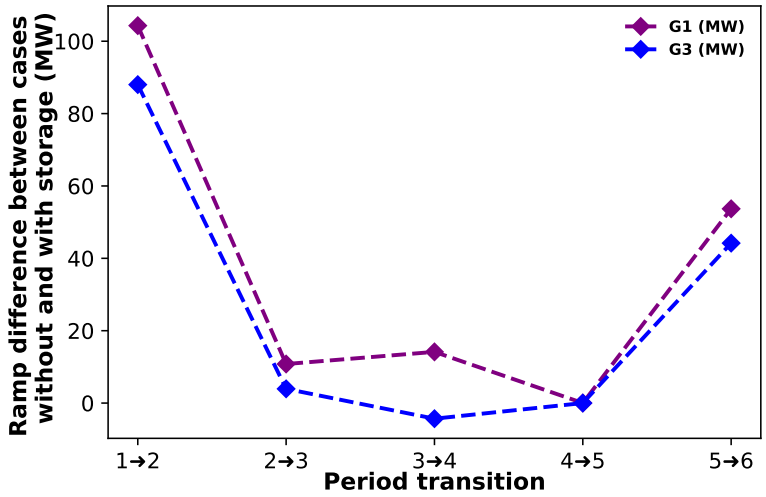

Figure 5: **5-Bus System** – Ramp difference. For each period, the left bar corresponds to the solution obtained while considering a storage device at bus 5, while the right bar corresponds to the same system without any storage device.

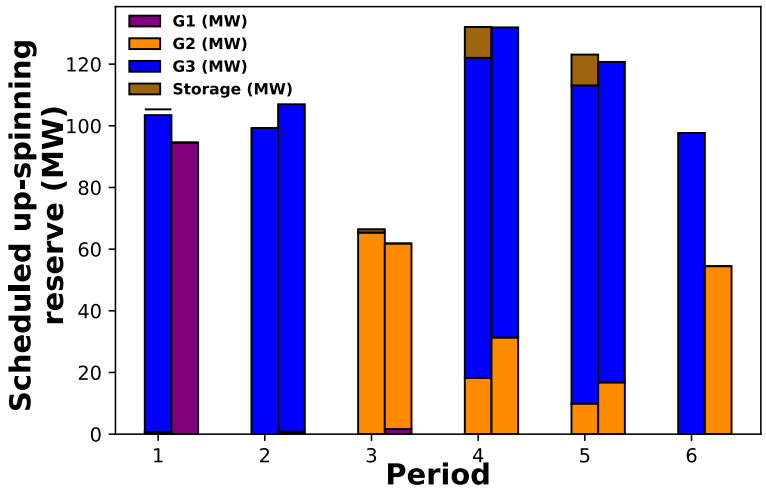

Figure 6: **5-Bus System** – Scheduled up-spinning reserve. For each period, the left bar corresponds to the solution obtained while considering a storage device at bus 5, while the right bar corresponds to the same system without any storage device.

same level of security in operations can be obtained with less commitment costs, less generation ramping as well as less conventional up-spinning reserves, respectively, during peak-hours when the storage device is present. Under a potential scenario where generator 1 (G1) fails and a given amount of renewable generation realizes, the systems can be re-dispatched as illustrated in Fig. 7. Note that both solutions would be able to supply demand. Nonetheless, when the storage is available, it reduces the stress of the system by providing power during the peak-hours. Overall, the total scheduling cost is $ 29870.78 without storage and $ 28883.43 with storage.

5.2. WECC-240 System

The WECC-240 test-system considered in this section comprises 240 buses, 448 transmission lines, 960 conventional generators (including hydro and biomass power plants), and 47 renewable units. For the numerical analysis, we consider a typical summer (August) day with total energy demand of approximately 1730

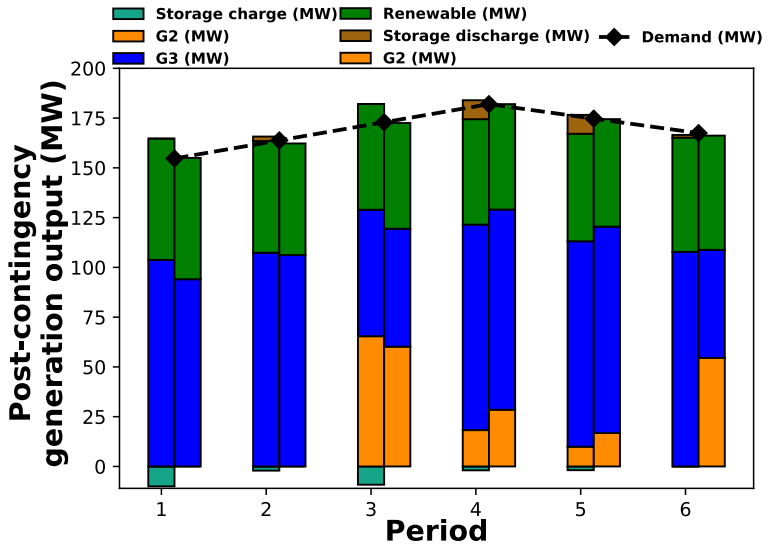

Figure 7: **5-Bus System** – Second stage post-contingency dispatch. For each period, the left bar corresponds to the solution obtained while considering a storage device at bus 5, while the right bar corresponds to the same system without any storage device.

GWh and an expected total renewable generation of roughly 267 GWh. In addition, we consider that storage devices are installed in 7 buses along the system and their combined capacity is equivalent to 3.1 GWh \ 2.05 GW. To characterize the renewable generation uncertainty of a typical August day in the West Coast of the US, we have collected 5 years (2015–2019) of solar and wind power production from the public database `https://www.renewables.ninja/` [42], providing us with 155 typical daily summer profiles. Each of these profiles was then considered as a potential scenario of real time renewable generation, following a data-driven decision-making structure. All data used in this numerical experiment can be found in [41].

Using the proposed methodology, we have obtained solutions of power and reserves scheduling for conventional and storage units under different modeling assumptions. The first solution is a base case where we analyze the scheduling under the nominal condition only, i.e., the scheduling of the first iteration of Algorithm 1 (hereinafter referred to as "solution iteration 0"). This scheduling does not take into account any information about the impact of vRES output variation or contingency states and therefore constitutes a deterministic solution. The second solution is obtained under the no-contingency assumption, i.e., by setting $K_g = 0$ in (46). This modeling assumption is hereinafter referred to as "solution $K_g = 0$". The third solution is similar to the "solution $K_g = 0$", but at most a single generator outage might occur, so it is called "solution $K_g = 1$ with storage". Finally, the fourth solution considers the single generator outage modeling assumption, but without the participation of storage devices. This solutions is hereinafter called "solution $K_g = 1$ without storage". In Table 1, we present the total scheduling (Column 2) and up/down reserve costs (Column 3 and Column 4) associated with each one of the aforementioned solutions, along with the respective total solution time. Furthermore, Figs. 8 and 9 depict the total scheduled hourly up-spinning and down-spinning reserves, respectively, for the single-outage-based ($K_g = 1$) solutions with and without the presence of storage devices, and Figs. 10 and 11 showcase the differences in the scheduled day-ahead ramping from coal and gas units for the same modeling assumptions as in Figs. 8 and 9.

Table 1: Total scheduling and up/down reserve costs for each obtained solution along with the respective total solution time.

Solution	**Total Cost ($)**			**Computing Time [s]**
	Scheduling	**Up Reserve**	**Down Reserve**	
Iteration 0	3664720.06	-	-	23.97
$K_g = 0$	3777031.85	90252.27	12934.63	12903.59
$K_g = 1$ **with storage**	3786216.78	101502.66	11495.84	26145.27
$K_g = 1$ **without storage**	3818669.34	103999.68	14002.21	25925.40

As expected, the cheapest total scheduling is associated with "solution iteration 0" (see Columns 2–4 in Table 1). In this modeling assumption, no up/down reserves are provisioned to be scheduled to cope with uncertainties related to vRES output or contingency states, therefore leaving the system vulnerable. Moreover, the second cheapest overall scheduling is from "solution $K_g = 0$", due to the lack of signaling against potential generation outages in the modeling, thus still leaving the system vulnerable to contingencies. Finally, the schedulings associated with the single-outage-based modeling assumptions, "solution $K_g = 1$ with storage" and "solution $K_g = 1$ without storage", are the most expensive among all modeling assumptions since they, essentially, provide the same level of security in operation as they are designed to withstand single contingency states and vRES output variation. It is interesting to note, nevertheless, that including storage devices decreases total scheduling costs as well as total costs of reserves. In fact, the decrease in up/down reserve prescription to system operator can also be seen in Figs. 8 and 9, where less total hourly up- and down-spinning reserves from conventional generators are needed when storage devices are considered. It is also worth mentioning that, from technical and operational viewpoints, storage devices significantly reduce the ramping of coal (during mid-day hours, e.g., Hour 12 and Hour 13) and gas generators during the peak hours (e.g., Hour 18 and Hour 19), when solar production uncertainty plays a significant role, as shown in Figs. 10 and 11.

5.3. Out-of-sample analysis

To evaluate the performance of the different modeling assumptions considered in this numerical experiment, we performed an out-of-sample analysis of the power and reserves scheduling for conventional and storage devices for each case. More specifically, we have generated a collection of 2000 out-of-sample scenarios of hourly system operation with the following procedure, aiming at emulating possible real-time *unseen* uncertainty realizations. On the one hand, for each out-of-sample scenario, a Bernoulli trial is sampled describing the availability state of each generator in the system, with *success* (trial equal to 1) standing for on-service and *fail* (trial equal to 0) for out-of-service state. For expository purposes and conservativeness in analysis, in these trials, we set the failure probability to 1%. On the other hand, to compose the out-of-sample scenario, we uniformly sample a renewable production profile from the dataset of 155 typical summer days collected from `RenewableNinja` public database. Fig. 12 depicts the inverse cumulative distribution among

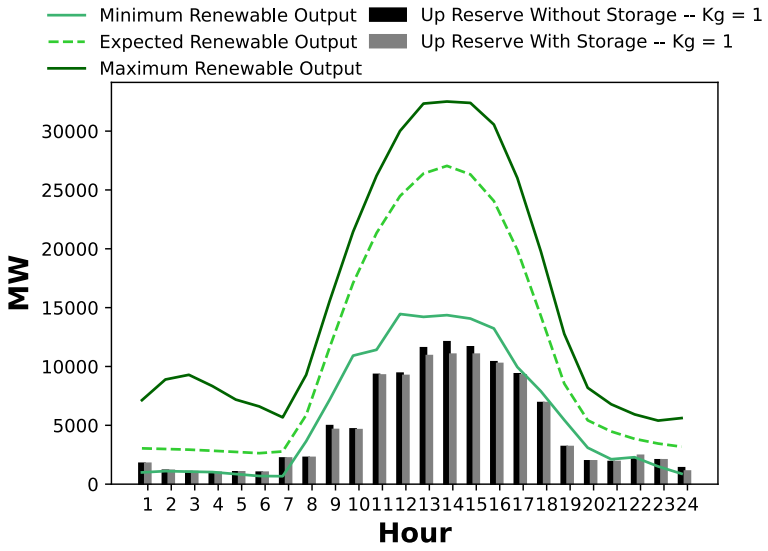

Figure 8: **WECC-240** – Total hourly up-spinning reserve for solutions "$K_g = 1$ without storage" and "$K_g = 1$ with storage".

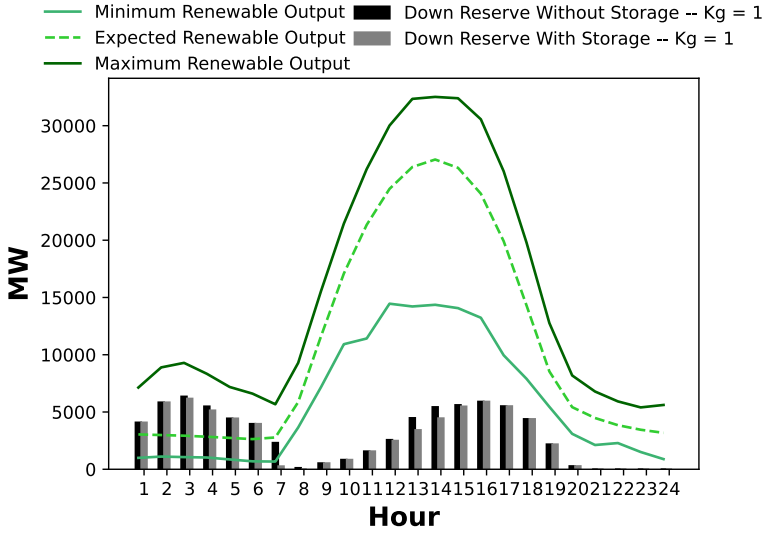

Figure 9: **WECC-240** – Total hourly down-spinning reserve for solutions "$K_g = 1$ without storage" and "$K_g = 1$ with storage".

the out-of-sample scenarios of negative imbalance at a peak hour (Hour 19) for the scheduling of the different modeling assumptions considered in this numerical experiment and Fig. 13 displays the hourly conditional expectation of negative imbalance over the out-of-sample scenarios that have at least one of the solutions with a negative imbalance strictly higher than zero. Furthermore, Fig. 14 showcases the hourly percentage of out-of-sample scenarios with negative imbalance higher than 1%, and Fig. 15 presents the hourly CVaR of negative imbalance for different the modeling assumptions.

In general, for all the considered evaluation metrics visually presented in Figs. 12–15, the base case (deterministic) "solution iteration 0" has the worst out-of-sample performance compared to "solution $K_g = 0$" and "solution $K_g = 1$ with storage". Notably, the highest levels of negative imbalance associated with "solution iteration 0" occur in the peak hours (middle of the day) as shown in Figs. 13 and 15. Moreover, compared to "solution iteration 0", by considering renewable uncertainty, "solution $K_g = 0$" achieves a better

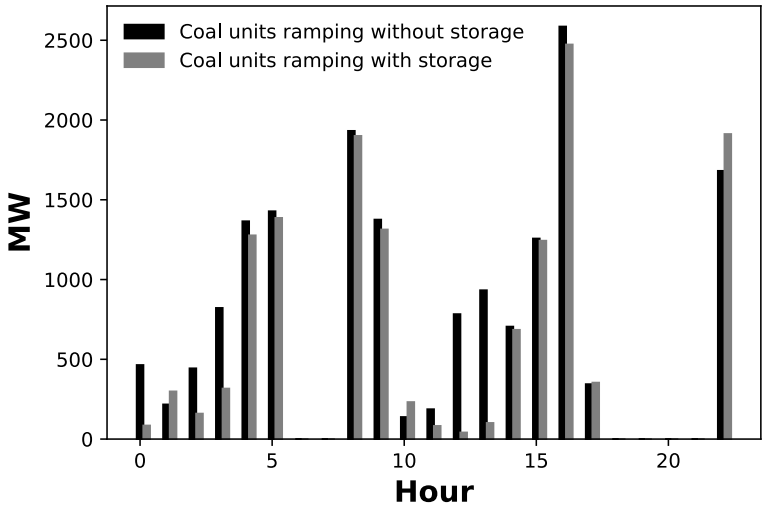

Figure 10: **WECC-240** – Hourly ramping (according to day-ahead scheduling) of coal generators for solutions "$K_g = 1$ without storage" and "$K_g = 1$ with storage".

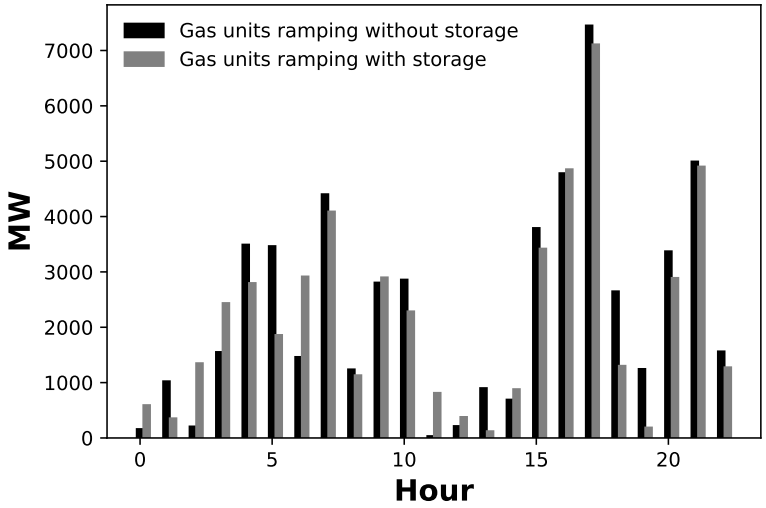

Figure 11: **WECC-240** – Hourly ramping (according to day-ahead scheduling) of gas generators for solutions "$K_g = 1$ without storage" and "$K_g = 1$ with storage".

performance with lower levels of negative imbalance. Nonetheless, the best overall performance is provided by the "solution $K_g = 1$ with storage" with the lowest number of scenarios with negative imbalance and lowest levels of negative imbalance of almost every hour. It is worth mentioning that we did not include the "solution $K_g = 1$ without storage" in this out-of-sample analysis as it attains similar results to those of the "solution $K_g = 1$ with storage". Nevertheless, it should be emphasized that this similar level of performance in the out-of-sample analysis comes at a lower total scheduling cost, as shown in Table 1, and with less afternoon ramping stress from conventional units, as demonstrated in Figs. 10 and 11. This effect highlights the capability of the proposed methodology of efficiently taking advantage of the benefits of storage devices to deliver a cheaper scheduling with the same level of out-of-sample performance.

Finally, as illustrated in Fig. 16, we performed an out-of-sample sensitivity analysis (similar to [43] but in a different context since here we see the problem from the market operator's perspective) on the parameter

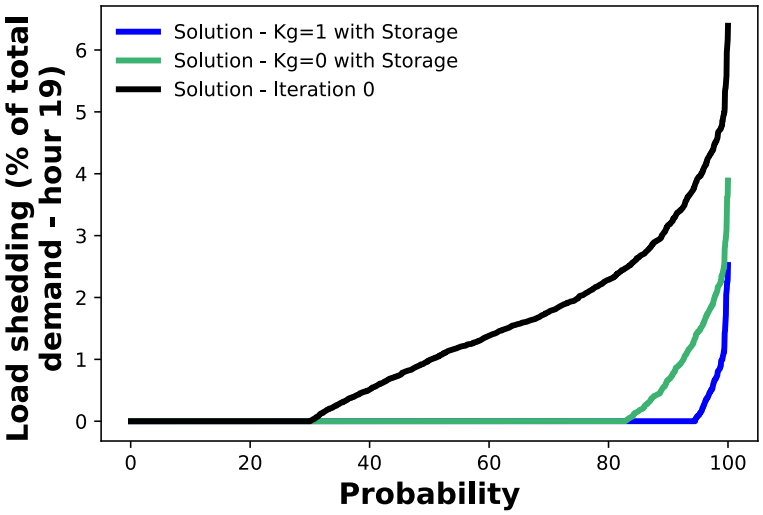

Figure 12: **WECC-240** – Inverse cumulative distribution of load shedding (or negative imbalance) at hour 19 for different solutions.

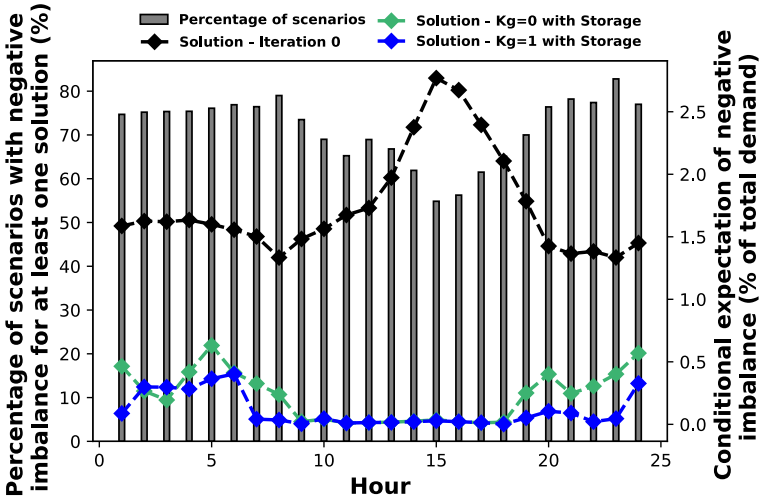

Figure 13: **WECC-240** – Conditional expectation of negative imbalance over scenarios that made at least one of the solutions incur in negative imbalance.

$\overline{\mathscr{L}}_t$ present in (16). Essentially, we solved the problem (1)–(16) three times. In each of these three times, we considered a different value for $\overline{\mathscr{L}}_t$ in constraint (16) and obtained a different scheduling solution. In addition, we tested each obtained solution in a simulation with 2000 scenarios of uncertainty realization following the same procedure utilized to obtain Fig. 12 and computed the CVaR of system imbalance for each of the different scheduling solutions. Values of total costs and CVaR associated with each scheduling solution are depicted in Fig. 16. As we can see, as we increase the allowed limit for CVaR of imbalance in (16), the total scheduling cost decreases, but the out-of-sample CVaR of load shedding tends to increase as expected.

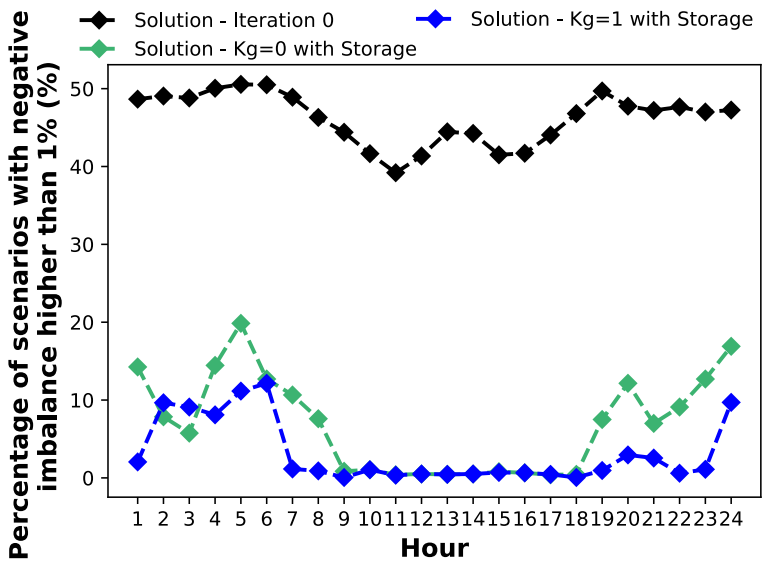

Figure 14: **WECC-240** – Percentage of scenarios with negative imbalance higher than 1% for each hour for different solutions.

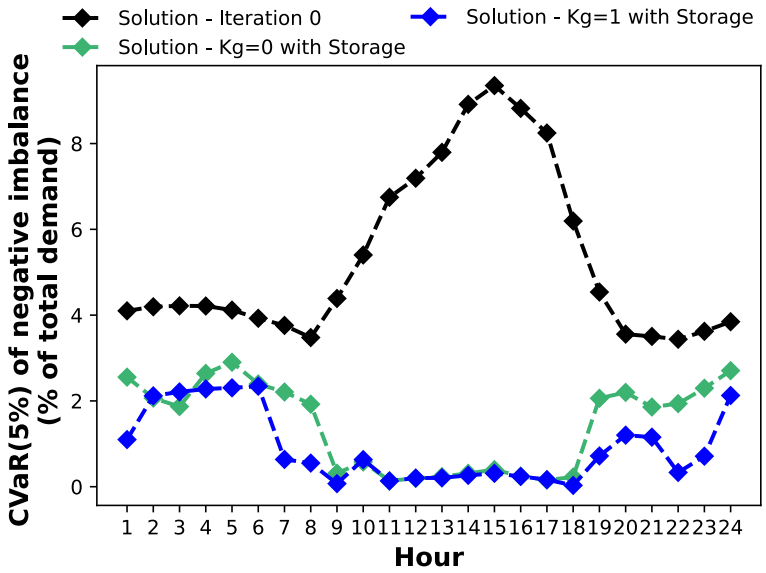

Figure 15: **WECC-240** – Hourly CVaR of negative imbalance for different solutions.

6. Conclusions

In this paper, we proposed a day-ahead CCUC methodology that properly captures the participation of BESSs to provide a cheaper scheduling of power and reserves while alleviating the ramping burden on conventional generators. Our modelling approach considers the participation of storage devices in assisting load following and post-contingency management as well as providing reserves alongside conventional units. The problem was formulated as a three-level system of mathematical programming models to obtain the least-cost scheduling while restricting the CVaR of the system-wide power imbalance to a user-defined tolerance level at each operating hour. To computationally handle the proposed formulation, we developed an efficient solution approach based on CCG techniques. We conducted two numerical experiments, one based on a

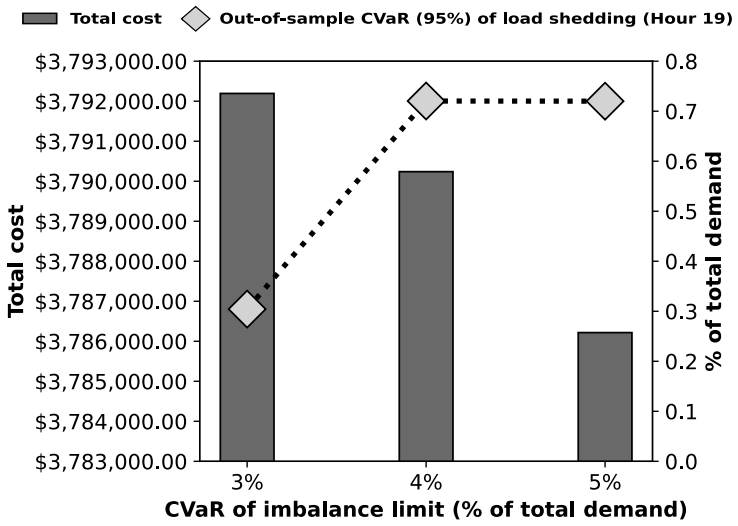

Figure 16: **WECC-240** – Out-of-sample sensitivity analysis on the parameter $\overline{\mathscr{L}}_t$ in (16). The horizontal axis has different values for $\overline{\mathscr{L}}_t$, the bars correspond to the left y-axis and the line corresponds to the right y-axis.

5-bus system and one based on the WECC-240 system aiming at empirically illustrating the capability of the proposed methodology to properly recognize the benefits of storage devices while planning the day-ahead scheduling. The key results indicate a reduction in the ramping rates of the conventional units in real-time operation and a better usage of the system resources, with a reduction in the overall system commitment levels and reserve scheduling costs when compared to close-related benchmarks. Future research will focus on the optimal placement of storage devices within our proposed framework to support the achievement of policy goals (e.g., full decarbonization) while keeping the operations of power systems secure.

Appendix A. Thermal Units Start-Up/Shut-Down Costs and Operating Constraints

In this appendix, for completeness purposes, the set that characterize the full formulation for the start-up/shut-down costs and operating constraints of each thermal unit $i \in \mathcal{I}$ used in this work in (16) is presented in (A.1)–(A.8).

$$\mathcal{U}_i = \left\{ \left(\boldsymbol{c}_i^{\mathrm{SU}}, \boldsymbol{c}_i^{\mathrm{SD}}, \boldsymbol{u}_i \right) \in \mathbb{R}_+^{|\mathcal{T}|} \times \mathbb{R}_+^{|\mathcal{T}|} \times \{0,1\}^{|\mathcal{T}|} \;\middle|\; \right.$$

$$\sum_{t=1}^{n_i^{UT}} (1 - u_{i,t}) = 0; \tag{A.1}$$

$$\sum_{t'=t}^{t+UT_i-1} u_{i,t'} \geq UT_i \left(u_{i,t} - u_{i,t-1} \right); \qquad \forall\, t \in \left\{ n_i^{UT} + 1, \ldots, |\mathcal{T}| - UT_i + 1 \right\} \tag{A.2}$$

$$\sum_{t'=t}^{|\mathcal{T}|} \left[u_{i,t'} - \left(u_{i,t} - u_{i,t-1} \right) \right] \geq 0; \qquad \forall\, t \in \left\{ |\mathcal{T}| - UT_i + 2, \ldots, |\mathcal{T}| \right\} \tag{A.3}$$

$$\sum_{t=1}^{n_i^{DT}} u_{i,t} = 0; \tag{A.4}$$

$$\sum_{t'=t}^{t+DT_i-1} (1-u_{i,t'}) \geq DT_i\big(u_{i,t-1}-u_{it}\big); \quad \forall\, t \in \big\{n_i^{DT}+1,\ldots,|\mathcal{T}|-DT_i+1\big\} \tag{A.5}$$

$$\sum_{t'=t}^{|\mathcal{T}|}\big[1-u_{i,t'}-\big(u_{i,t-1}-u_{i,t}\big)\big] \geq 0; \qquad \forall\, t \in \big\{|\mathcal{T}|-DT_i+2,\ldots,|\mathcal{T}|\big\} \tag{A.6}$$

$$c_{i,t}^{\mathrm{SU}} \geq C_{i,t}^{\mathrm{SU}}\big(u_{i,t}-u_{i,t-1}\big); \qquad \forall\, t \in \mathcal{T} \tag{A.7}$$

$$c_{i,t}^{\mathrm{SD}} \geq C_{i,t}^{\mathrm{SD}}\big(u_{i,t-1}-u_{i,t}\big); \qquad \forall\, t \in \mathcal{T} \Big\}. \tag{A.8}$$

where, $n_i^{DT} = \min\big\{|\mathcal{T}|, \big(DT_i - n_{i,0}^{off}\big)\big(1-V_{i,0}\big)\big\}$ and $n_i^{UT} = \min\big\{|\mathcal{T}|, \big(UT_i - n_{i,0}^{on}\big)V_{i,0}\big\}$. We refer to [32] for a wide discussion on the correctness and computational effectiveness of formulation (A.1)–(A.8).

References

[1] REN21, Renewables 2017 – Global Status Report, Tech. rep., REN21 Secretariat (2017).

[2] T. Kåberger, Progress of Renewable Electricity Replacing Fossil Fuels, Global Energy Interconnection 1 (1) (2018) 48–52. doi:10.14171/j.2096-5117.gei.2018.01.006.

[3] F. Slye, Future Energy Scenarios, Tech. rep., National Grid (Jul 2018).

[4] M. Nyberg – California Energy Commission, Thermal Efficiency of Natural Gas-Fired Generation in California: 2019 Update (2020).

[5] Senate Bill No. 100, accessed: 30-07-2020 (2018).
URL `https://leginfo.legislature.ca.gov/faces/billTextClient.xhtml?bill_id=201720180SB100.`

[6] M. Picker, Decision Adopting Preferred System Portfolio and Plan for 2017-2018 Integrated Resource Plan Cycle (2019).

[7] S. Chen, Z. Li, W. Li, Integrating High Share of Renewable Energy into Power System using Customer-Sited Energy Storage, Renewable and Sustainable Energy Reviews 143 (2021) 110893. doi:10.1016/j.rser.2021.110893.

[8] G. Haddadian, N. Khalili, M. Khodayar, M. Shahidehpour, Optimal scheduling of distributed battery storage for enhancing the security and the economics of electric power systems with emission constraints, Electric Power Systems Research 124 (2015) 152–159. doi:https://doi.org/10.1016/j.epsr.2015.03.002.
URL `https://www.sciencedirect.com/science/article/pii/S0378779615000620`

[9] A. Ghasempour, Advanced Metering Infrastructure in Smart Grid: Requirements, Challenges, Architectures, Technologies, and Optimizations (08 2017).

[10] D. Pozo, J. Contreras, E. E. Sauma, Unit Commitment with Ideal and Generic Energy Storage Units, IEEE Transactions on Power Systems 29 (6) (2014) 2974–2984. doi:10.1109/TPWRS.2014.2313513.

[11] R. Sioshansi, Using Storage-Capacity Rights to Overcome the Cost-Recovery Hurdle for Energy Storage, IEEE Transactions on Power Systems 32 (3) (2017) 2028–2040. doi:10.1109/TPWRS.2016.2607153.

[12] H. Follmer, A. Schied, Stochastic Finance: An Introduction in Discrete Time, 3rd Edition, De Gruyter, 2011.

[13] B. Zeng, L. Zhao, Solving Two-Stage Robust Optimization Problems using a Column-and-Constraint Generation Method, Operations Research Letters 41 (5) (2013) 457–461.

[14] L. A. Roald, D. Pozo, A. Papavasiliou, D. K. Molzahnd, J. Kazempour, A. Conejo, Power Systems Optimization under Uncertainty: A Review of Methods and Applications, Electric Power Systems Research 214 – Part A (2023) 108725. doi:10.1016/j.epsr.2022.108725.

[15] M. Eslahi, A. F. Nematollahi, B. Vahidi, Day-Ahead Scheduling of Centralized Energy Storage System in Electrical Networks by Proposed Stochastic MILP-Based Bi-Objective Optimization Approach, Electric Power Systems Research 192 (2021) 106915. doi:https://doi.org/10.1016/j.epsr.2020.106915.

[16] P. Liang, N. Bohlooli, Optimal Unit Commitment Integrated Energy Storage System, Renewable Energy

Sources and FACTS Devices with Robust Method, Electric Power Systems Research 209 (2022) 107961. doi:https://doi.org/10.1016/j.epsr.2022.107961.

[17] Y. Wen, C. Guo, D. S. Kirschen, S. Dong, Enhanced Security-Constrained OPF with Distributed Battery Energy Storage, IEEE Transactions on Power Systems 30 (1) (2015) 98–108. doi:10.1109/TPWRS.2014.2321181.

[18] Y. Wen, C. Guo, H. Pandzic, D. S. Kirschen, Enhanced Security-Constrained Unit Commitment with Emerging Utility-Scale Energy Storage, IEEE Transactions on Power Systems 31 (1) (2016) 652–662. doi:10.1109/TPWRS.2015.2407054.

[19] Y. Chen, R. Baldick, Battery Storage Formulation and Impact on Day Ahead Security Constrained Unit Commitment, IEEE Transactions on Power Systems 37 (5) (2022) 3995–4005. doi:10.1109/TPWRS.2022.3144241.

[20] A. Street, A. Brigatto, D. M. Valladão, Co-Optimization of Energy and Ancillary Services for Hydrothermal Operation Planning Under a General Security Criterion, IEEE Transactions on Power Systems 32 (6) (2017) 4914–4923. doi:10.1109/TPWRS.2017.2672555.

[21] L. Silva-Rodriguez, A. Sanjab, E. Fumagalli, M. Gibescu, Light Robust Co-Optimization of Energy and Reserves in the Day-Ahead Electricity Market, Applied Energy 353 (2024) 121982. doi:https://doi.org/10.1016/j.apenergy.2023.121982.
URL https://www.sciencedirect.com/science/article/pii/S0306261923013466

[22] M. Mehrtash, B. F. Hobbs, E. Ela, Reserve and Energy Scarcity Pricing in United States Power Markets: A Comparative Review of Principles and Practices, Renewable and Sustainable Energy Reviews 183 (2023) 113465. doi:https://doi.org/10.1016/j.rser.2023.113465.
URL https://www.sciencedirect.com/science/article/pii/S1364032123003222

[23] X. Qin, B. Xu, I. Lestas, Y. Guo, H. Sun, The Role of Electricity Market Design for Energy Storage in Cost-Efficient Decarbonization, Joule 7 (6) (2023) 1227–1240. doi:https://doi.org/10.1016/j.joule.2023.05.014.
URL https://www.sciencedirect.com/science/article/pii/S2542435123002118

[24] Y. Huang, D. Gordon, P. Scott, Receding Horizon Dispatch of Multi-Period Look-Ahead Market for Energy Storage Integration, Applied Energy 352 (2023) 121856. doi:https://doi.org/10.1016/j.apenergy.2023.121856.
URL https://www.sciencedirect.com/science/article/pii/S0306261923012205

[25] Y. Liu, L. Wu, Y. Yang, Y. Chen, R. Baldick, R. Bo, Secured Reserve Scheduling of Pumped-Storage Hydropower Plants in ISO Day-Ahead Market, IEEE Transactions on Power Systems 36 (6) (2021) 5722–5733. doi:10.1109/TPWRS.2021.3077588.

[26] Z. Tang, Y. Liu, L. Wu, J. Liu, H. Gao, Reserve Model of Energy Storage in Day-Ahead Joint Energy and Reserve Markets: A Stochastic UC Solution, IEEE Transactions on Smart Grid 12 (1) (2021) 372–382. doi:10.1109/TSG.2020.3009114.

[27] Y. Zhou, Q. Zhai, L. Wu, Multistage Transmission-Constrained Unit Commitment With Renewable Energy and Energy Storage: Implicit and Explicit Decision Methods, IEEE Transactions on Sustainable Energy 12 (2) (2021) 1032–1043. doi:10.1109/TSTE.2020.3031054.

[28] L. Baringo, M. Carrión, R. Domínguez, Day-Ahead Market Scheduling Considering Renewable Energies, Springer International Publishing, Cham, 2023, pp. 151–193.

[29] N. E. Koltsaklis, J. Knapek, Assessing Flexibility Options in Electricity Market Clearing, Renewable and Sustainable Energy Reviews 173 (2023) 113084. doi:https://doi.org/10.1016/j.rser.2022.113084.

[30] M. Zhang, Z. Jiao, L. Ran, Y. Zhang, Optimal Energy and Reserve Scheduling in a Renewable-Dominant Power System, Omega 118 (2023) 102848. doi:https://doi.org/10.1016/j.omega.2023.102848.

[31] D. Woodfin, C. V. Seely, NPRR 1186 – Improvements Prior to the RTC+B Project for Better ESR State of Charge Awareness, Accounting, and Monitoring, 2023.

[32] M. Carrión, J. M. Arroyo, A Computationally Efficient Mixed-Integer Linear Formulation for the Thermal Unit Commitment Problem, IEEE Trans. Power Syst. 21 (3) (2006) 1371–1378. doi:10.1109/TPWRS.2006.876672.

[33] R. Hettich, K. O. Kortanek, Semi-Infinite Programming: Theory, Methods, and Applications, SIAM Review 35 (3) (1993) 380–429.

[34] B. Fanzeres, S. Ahmed, A. Street, Robust Strategic Bidding in Auction-Based Markets, European Journal of Operational Research 272 (3) (2019) 1158–1172.

[35] B. Fanzeres, A. Street, D. Pozo, A Column-and-Constraint Generation Algorithm to Find Nash Equilibrium in Pool-Based Electricity Markets, Electric Power Systems Research 189 (2020) 106806.

[36] A. Moreira, B. Fanzeres, G. Strbac, Energy and Reserve Scheduling under Ambiguity on Renewable Probability Distribution, Electric Power Systems Research 160 (2018) 205–218.

[37] A. Gupte, S. Ahmed, M. S. Cheon, S. Dey, Solving Mixed Integer Bilinear Problems using MILP Formulations, SIAM Journal on Optimization 23 (2) (2013) 721–744.

[38] A. Moreira, G. Strbac, B. Fanzeres, An Ambiguity Averse Approach for Transmission Expansion Planning, in: Proceedings of the IEEE PowerTech 2019, 2019, pp. 1–6.

[39] J. E. Price, J. Goodin, Reduced Network Modeling of WECC as a Market Design Prototype, in: 2011 IEEE PES General Meeting, 2011, pp. 1–6. doi:10.1109/PES.2011.6039476.

[40] A. Street, F. Oliveira, J. M. Arroyo, Contingency-Constrained Unit Commitment with $n-K$ Security Criterion: A Robust Optimization Approach, IEEE Transactions on Power Systems 26 (3) (2011) 1581–1590. doi:10.1109/TPWRS.2010.2087367.

[41] Dataset used in the case studies.
URL `https://bit.ly/3FtSMzc`

[42] I. Staffell, S. Pfenninger, Using Bias-Corrected Reanalysis to Simulate Current and Future Wind Power Output, Energy 114 (2016) 1224–1239.

[43] E. D. Castronuovo, J. Usaola, R. Bessa, M. Matos, I. Costa, L. Bremermann, J. Lugaro, G. Kariniotakis, An integrated approach for optimal coordination of wind power and hydro pumping storage, Wind Energy 17 (6) (2014) 829–852. arXiv:https://onlinelibrary.wiley.com/doi/pdf/10.1002/we.1600, doi:https://doi.org/10.1002/we.1600.
URL `https://onlinelibrary.wiley.com/doi/abs/10.1002/we.1600`